CP violation in top quark pair production at hadron colliders

Hong-Yi Zhou
*Institute of Modern Physics and Department of Physics, Tsinghua University, Beijing 100084, People's Republic of China and Institut für Theoretische Physik, Universität Heidelberg, Philosophenweg 16, D-69120 Heidelberg, Germany**
(Received 20 May 1998; published 13 October 1998)

CP violating effects in top quark pair production at the future 2 TeV $p\bar{p}$ Fermilab Tevatron and 14 TeV pp CERN LHC colliders are investigated. We study three kinds of *CP* violating sources: the supersymmetric *CP*-odd phase of the top squark trilinear soft breaking term arg(A_t), the *CP*-odd parameter in two-Higgs-doublet extensions of the standard model (2HDM), and the model-independent top quark chromoelectric dipole moment (CEDM), respectively. Optimal observables as well as simple observables are used. We find that it is possible to observe *CP* violating effects from arg(A_t) in top quark pair production at the 2 TeV Fermilab Tevatron with ~ 30 fb^{-1} integrated luminosity when $m_{\tilde{g}} \sim 200$ GeV. If the experimental systematic errors are sufficiently small, the CERN LHC with ~ 150 fb^{-1} can put a limit of order 10^{-1} on the phase arg(A_t) and the *CP*-odd parameter in 2HDM by using optimal observables. The CEDM of the top quark can be measured to an accuracy of 10^{-18} cm g_s at the Fermilab Tevatron and few $\times 10^{-20}$ cm g_s at the CERN LHC. [S0556-2821(98)07119-7]

PACS number(s): 14.65.Ha, 11.30.Er, 12.38.Bx

I. INTRODUCTION

At the future hadron colliders such as the upgraded Fermilab Tevatron with $\sqrt{s}=2$ TeV and the CERN Large Hadron Collider (LHC) with $\sqrt{s}=14$ TeV, the annual top quark pair yields are about 7×10^4 (with integrated luminosity $\int \mathcal{L}=10$ fb^{-1}) and 7×10^7 (with $\int \mathcal{L}=100$ fb^{-1}), respectively. The large numbers of top quark pairs allow us to do precise measurements on physical quantities associated with the top quark. Among them are the production cross sections, the top quark mass, and the discrete symmetry properties. Because of the QCD uncertainties and the experimental systematic errors, the precision of cross section measurement is only about 5%–6% [1]. The discrete symmetry properties such as parity nonconservation and *CP* violation do not suffer from QCD background uncertainty and their accuracies of measurements depend mainly on the statistical errors provided the experimental systematic errors are sufficiently small. Therefore the discrete symmetry properties can be measured more precisely than the cross sections. New physics which has no observable contributions to the cross section may have observable effects in parity or *CP* violation. Since the standard model (SM) contributions to parity violation [2] and *CP* violation are small, possible observed large effects of them will reveal new physics.

In a previous work [3], we have shown that the minimal supersymmetric (SUSY) extension of the standard model (MSSM) [4] gives observable parity violating effects at the Fermilab Tevatron while its corrections to the production cross section are within the QCD theorectical uncertainties. In this paper, we shall concentrate on the *CP*-violating effects induced by nonstandard model interactions. We investigate three kinds of *CP*-violating sources: the supersymmetric *CP*-odd phase of the top squark trilinear soft breaking term arg(A_t), the *CP*-odd parameter in two-Higgs-doublet extensions of the standard model (2HDM), and the model-independent top quark chromoelectric dipole moment (CEDM), respectively. In the MSSM, *CP* violation exists in strong interaction and in the 2HDM, *CP* violation can have strong Yukawa couplings because of the heavy top quark mass. Therefore, both can produce possible large effects. It is also useful to study *CP* violation in a model-independent way when we do not know what is the new physics. *CP* violation in top quark pair production at hadron colliders is also studied in Refs. [5–14]. In Ref. [7], SUSY QCD *CP* violating effects are studied in the $gg\to t\bar{t}$ process by using a charge energy asymmetry observable that is only sensitive to the imaginary part of the loop integrals. In this work, we use the optimal observables as well as naive observables constructed from the final state momenta. Possible large *CP* violating effects in 2HDM and the methods of observing them in top quark pair production at hadron colliders are studied in Refs. [6,12]. We extend those studies by applying optimal observables. In Ref. [8], the method of extracting real top quark CEDM in the reaction $gg\to t\bar{t}$ is studied. It is found that the optimal observables are particularly effective. We include here an imaginary part of CEDM and the reaction $q\bar{q}\to t\bar{t}$ at the Fermilab Tevatron. Furthermore, we use the exact amplitudes of $gg(q\bar{q})\to t\bar{t}\to bl_1^+\nu_{l_1}\bar{b}l_2^-\bar{\nu}_{l_2}$ ($b\bar{q}_1q_1'\bar{b}q_2\bar{q}_2'$). In Ref. [8], the top quark spin in its rest frame is taken to be in the direction of the lepton. This is a kind of approximation, although the lepton is a good analyzer of the top quark spin, because in the top rest frame, the lepton momentum has the angular distribution proportional to $1+\cos\psi$ with ψ being the angle between the top spin and the lepton momentum. The possibility of using polarized proton was studied in Ref. [14].

In Sec. II, we describe the models and the calculations. The methods of extracting *CP*-violating effects are given in Sec. III. In Sec. IV, we present our results, discussions, and conclusions.

*Mailing address.

II. MODELS AND CALCULATIONS

A. *CP* violation in MSSM

In the MSSM, two possibilities can induce CP violation in top quark interactions: the complex phase in Higgs boson mass parameter μ, and the complex phase in scalar top supersymmetric soft breaking trilinear coupling A_t. The experimental limit on the neutron electric dipole moment (NEDM), $d_n \leqslant 1.1\times 10^{-25} e-cm$ [15], places a severe constraint on the phase of μ. Therefore, the only significant SUSY CP-odd phase in association with the top quark is $\arg(A_t)$. In Ref. [16], it is argued that the phase $\arg(A_t)$ is not strongly constrained by current experiments and the effects in single top quark production and decay are studied. In this work, we shall assume $\arg(\mu)=0$ and let $\arg(A_t)$ be a free parameter of no *a priori* constraints.

The parameter $\arg(A_t)$ enters in the scalar top quark mixing. The mass eigenstates $\tilde{t}_1$ and $\tilde{t}_2$ of scalar top quark are related to the current eigenstates $\tilde{t}_L$ and $\tilde{t}_R$ by

$$\tilde{t}_1=\tilde{t}_L\cos\ \theta_t+\tilde{t}_R\sin\ \theta_t e^{-i\beta_t},$$

$$\tilde{t}_2=-\tilde{t}_L\sin\ \theta_t e^{i\beta_t}+\tilde{t}_R\cos\ \theta_t. \tag{1}$$

The mixing angle θ_t, phase β_t as well as the masses $m_{\tilde{t}_{1,2}}$ can be calculated by diagonalizing the following mass matrix [4] :

$$M_{\tilde{t}}^2=\begin{pmatrix} M_{\tilde{t}_L}^2 & m_t m_{LR}^{\star} \\ m_t m_{LR} & M_{\tilde{t}_R}^2 \end{pmatrix},$$

$$M_{\tilde{t}_L}^2=m_{\tilde{t}_L}^2+m_t^2+(\tfrac{1}{2}-\tfrac{2}{3}\sin^2\theta_W)\cos(2\beta)m_Z^2,$$

$$M_{\tilde{t}_R}^2=m_{\tilde{t}_R}^2+m_t^2+\frac{2}{3}\sin^2\theta_W\cos(2\beta)m_Z^2,$$

$$m_{LR}=-\mu\ \cot\ \beta-A_t, \tag{2}$$

where $m_{\tilde{t}_L}^2$, $m_{\tilde{t}_R}^2$ are the soft SUSY-breaking mass terms of left- and right-handed top squarks, $\tan\beta=v_2/v_1$ is the ratio of the vacuum expectation values of the two Higgs doublets.

From Eqs. (1) and (2), we can get the expressions for $m_{\tilde{t}_{1,2}}^2$, θ_t, and β_t:

$$m_{\tilde{t}_{1,2}}^2=\frac{1}{2}[M_{\tilde{t}_L}^2+M_{\tilde{t}_R}^2\mp\sqrt{(M_{\tilde{t}_L}^2-M_{\tilde{t}_R}^2)^2+4m_t^2|m_{LR}|^2}], \tag{3}$$

$$\tan\ \theta_t=\frac{m_{\tilde{t}_1}^2-M_{\tilde{t}_L}^2}{m_t(-\mu\ \cot\ \beta-|A_t|\cos\ \theta_{A_t})}\cos\ \beta_t, \tag{4}$$

$$\tan\ \beta_t=\frac{|A_t|\sin\ \theta_{A_t}}{\mu\ \cot\ \beta+|A_t|\cos\ \theta_{A_t}}, \tag{5}$$

where $\theta_{A_t}=\arg(A_t)$.

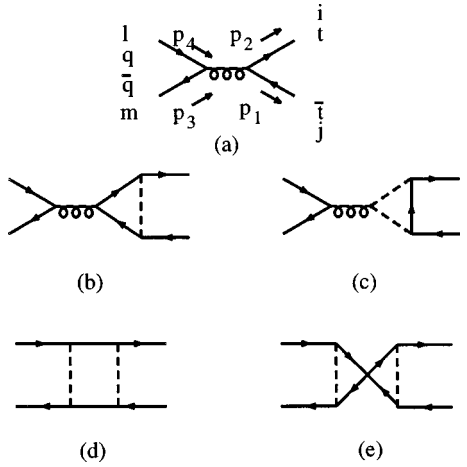

FIG. 1. Feynman diagrams of tree-level and 1-loop SUSY QCD corrections of CP violation to $q\bar{q}\to t\bar{t}$.

In the presence of squark mixing,the strong squark-quark-gluino interaction Lagrangian is given by

$$L_{\tilde{g}\tilde{q}\bar{q}}=-g_s T_{jk}^a\bar{q}_k[(a_1-b_1\gamma_5)\tilde{q}_{1j}+(a_2-b_2\gamma_5)\tilde{q}_{2j}]\tilde{g}_a+\text{H.c.}, \tag{6}$$

where g_s is the strong coupling constant, T^a are $\mathrm{SU}(3)_C$ generators, and for the top quark a_1, b_1, a_2, b_2 are given by

$$a_1=\frac{1}{\sqrt{2}}(\cos\ \theta_t-\sin\ \theta_t e^{i\beta_t}),$$

$$b_1=-\frac{1}{\sqrt{2}}(\cos\ \theta_t+\sin\ \theta_t e^{i\beta_t}),$$

$$a_2=-\frac{1}{\sqrt{2}}(\cos\ \theta_t+\sin\ \theta_t e^{-i\beta_t}),$$

$$b_2=-\frac{1}{\sqrt{2}}(\cos\ \theta_t-\sin\ \theta_t e^{-i\beta_t}). \tag{7}$$

The above interactions enter in the virtual corrections to the main production processes of $t\bar{t}$ at hadron colliders: $q\bar{q}\to t\bar{t}$ and $gg\to t\bar{t}$. There are also weak squark-quark-neutralino and squark-quark-chargino interactions. Since their coupling constants are an order of magnitude smaller than the strong SUSY QCD squark-quark-gluino interaction, we shall not consider them here. However, they may be important when the main processes are weak interactions [16].

In Figs. 1(a)–(e), the Feynman diagrams of the QCD tree-level and SUSY QCD virtual corrections of the process $q\bar{q}\to t\bar{t}$ are given. The corresponding Feynman diagrams of $gg\to t\bar{t}$ are presented in Figs. 2(a)–(m) [the u channels of Figs. 2(b), (f)–(m) are not depicted]. The dashed lines in the loop stand for scalar quarks, while the solid lines for gluinos. In Ref. [7], CP-violating effects are studied using a charge energy asymmetry observable which is only sensitive to the

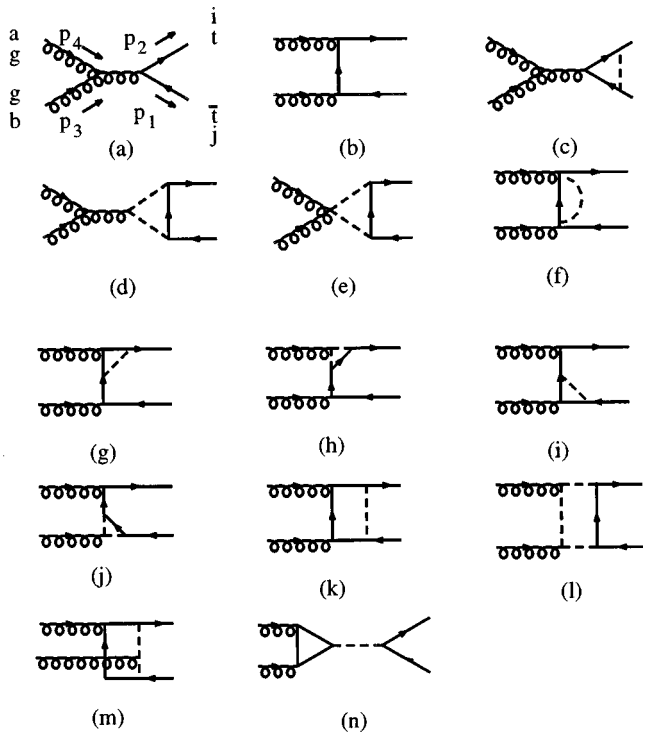

FIG. 2. Feynman diagrams of tree-level and 1-loop SUSY QCD corrections of *CP* violation to $gg\to t\bar{t}$.

imaginary part of the loop integrals. Therefore, there are no contributions to the charge energy asymmetry from Figs. 2(f)–(j),(m).

The one loop scattering amplitudes of $q\bar{q}\to t\bar{t}$ and $gg\to t\bar{t}$ were already presented in Refs. [17–19] for calculating the total production rates of $t\bar{t}$ pairs. To calculate the *CP*-violating effects in the $t\bar{t}$ system, additional renormalized amplitudes are needed. In terms of the tree-level amplitude M_0^a and the next-to-leading order SUSY QCD corrections δM^a, the renormalized amplitudes of $a\bar{a}\to t\bar{t}$ ($a=q,\ g$) at the one-loop level may be written as

$$M^a = M_0^a + \delta M^a, \tag{8}$$

where δM^a can be decomposed into two parts: δM^{aS} which contains even combination of γ_5 and $\epsilon_{\mu\nu\rho\sigma}$, and δM^{aA} containing odd combination of γ_5 and $\epsilon_{\mu\nu\rho\sigma}$. The symmetry breaking effects are contained in δM^{aA} which has no contributions to the total cross sections at next-to-leading order, while δM^{aS} will contribute to the total cross sections. We shall assume that δM^{aS} is small enough to be within the 5 %–6 % uncertainty and therefore is neglected in our calculations. We also discard terms in δM^{aA} which give only parity asymmetry [3].

Let us denote the momenta of the initial and the final state particles as $a(p_4)\bar{a}(p_3)\to t_i(p_2)\bar{t}_j(p_1)$. We may use, as a further shorthand, the notation for $a=q$ that $u_i \equiv u(p_i)$($v_i \equiv v(p_i)$) denotes the Dirac four-spinor corresponding to the momentum and spin of particle (antiparticle). When $a=g$ we use $\epsilon_i \equiv \epsilon(p_i)$ for the gluon polarization function. In this notation, the tree-level amplitude for $a=q$ can be written as

$$M_0^q = ig_s^2 (T_{ji}^c T_{lm}^c)\bar{v}_3 \gamma^\mu u_4 \bar{u}_2 \gamma_\mu v_1 / \hat{s}, \tag{9}$$

where $\hat{s}$ is the invariant mass of the $t\bar{t}$ pair.

The tree-level amplitude for $a=g$ is composed of three different production channels (s,t,u channel) as follows:

$$\begin{aligned} M_0^{gs} &= -ig_s^2 (if_{abc}T^c)_{ji}\bar{u}(p_2)\Gamma v(p_1)/\hat{s} \\ &= -ig_s^2 (T^a T^b - T^b T^a)_{ji} M_0^s, \end{aligned} \tag{10}$$

$$\begin{aligned} M_0^{gt} &= -ig_s^2 (T^b T^a)_{ji}\bar{u}(p_2)\epsilon\!\!\!/_4 (q\!\!\!/ + m_t)\epsilon\!\!\!/_3 v(p_1)/(\hat{t}-m_t^2) \\ &= -ig_s^2 (T^b T^a)_{ji} M_0^t, \end{aligned} \tag{11}$$

$$\begin{aligned} M_0^{gu} &= M_0^{gt}(p_3 \leftrightarrow p_4, \quad T^a \leftrightarrow T^b, \quad \hat{t}\to\hat{u}) \\ &= -ig_s^2 (T^a T^b)_{ji} M_0^u, \end{aligned} \tag{12}$$

where $q=p_2-p_4$, Γ^μ is given in Appendix A.

To calculate the *CP*-violating effects induced by the SUSY QCD effects, we follow the method presented in Refs. [5,20], in which the amplitudes were calculated numerically using the helicity amplitude method. To obtain the renormalized scattering amplitudes, we adopt the dimensional regularization scheme to regulate the ultraviolet divergences and the on-mass-shell renormalization scheme to subtract the divergences [21].

The SUSY QCD corrections to the scattering amplitude δM^{aA} for $a=q$ arise from the vertex diagram, the box diagram, as well as the crossed-box diagram. The renormalized amplitudes can be written as

$$\delta M^{qA} = \delta M^{qv} + \delta M^{DB} + \delta M^{CB}, \tag{13}$$

where δM^{qv} is the vertex corrections of Figs. 1(b) and (c), and δM^{DB} and δM^{CB} are the contributions from the box diagram and crossed-box diagram of Figs. 1(d) and (e), respectively. The results for these separate contributions are

$$\delta M^{qv} = ig_s^2 (T_{ji}^c T_{lm}^c)\bar{v}_3 (p\!\!\!/_2 - p\!\!\!/_1) u_4 \bar{u}_2 (-D^s \gamma_5) v_1 / \hat{s}, \tag{14}$$

$$\delta M^{DB} = ig_s^{2\,7}_{\,6} (T_{ji}^c T_{lm}^c) f^{DB} [\bar{u}_2 p\!\!\!/_3 \gamma_5 u_4 \bar{v}_3 v_1 - \bar{u}_2 p\!\!\!/_3 u_4 \bar{v}_3 \gamma_5 v_1 + \bar{u}_2 u_4 \bar{v}_3 p\!\!\!/_4 \gamma_5 v_1 + \bar{u}_2 \gamma_5 u_4 \bar{v}_3 p\!\!\!/_4 v_1], \tag{15}$$

$$\delta M^{CB} = \frac{2}{7}\delta M^{DB}(p_3 \leftrightarrow p_4). \tag{16}$$

The form factor D^s corresponding to the top quark CEDM and the form factor f^{DB} are given in Appendix A.

The SUSY QCD corrections to the scattering amplitude δM^{gA} of $gg\to t\bar{t}$ can be written as

$$\delta M^{gA}_{ji} = -ig_s^2(\delta M^+ O^{(+)}_{ji} + \delta M^- O^{(-)}_{ji} + \delta M^\delta [\delta_{ab}]_{ji}), \tag{17}$$

with

$$O^{(+)} = \frac{T^a T^b + T^b T^a}{2}, \quad O^{(-)} = \frac{T^b T^a - T^a T^b}{2}, \tag{18}$$

$$\delta M^+ = -\tfrac{1}{3}\delta M^{s2} + \delta M^{\mathrm{self},t} + \delta M^{\mathrm{self},u} + \delta M^{v1,t} + \delta M^{v1,u} + \delta M^{v2,t} + \delta M^{v2,u} + \delta M^{\mathrm{box1},t} + \delta M^{\mathrm{box1},u} + \delta M^{\mathrm{box2},t} + \delta M^{\mathrm{box2},u},$$

$$\delta M^- = -2\delta M^{s1} + \delta M^{\mathrm{self},t} - \delta M^{\mathrm{self},u} + \delta M^{v1,t} - \delta M^{v1,u} + \delta M^{v2,t} - \delta M^{v2,u} + \delta M^{\mathrm{box1},t} - \delta M^{\mathrm{box1},u} + \delta M^{\mathrm{box2},t} - \delta M^{\mathrm{box2},u},$$

$$\delta M^\delta = \tfrac{1}{2}\delta M^{s2} + \tfrac{1}{6}(\delta M^{\mathrm{box1},t} + \delta M^{\mathrm{box1},u}) - \tfrac{3}{2}(\delta M^{\mathrm{box2},t} + \delta M^{\mathrm{box2},u}) - (\delta M^{\mathrm{box3},t} + \delta M^{\mathrm{box3},u}). \tag{19}$$

In the above expressions, the superscript t,u stand for t,u channel. δM^{s1} is the s channel vertex corrections from Figs. 2(c) and (d), δM^{s2} from (e), $\delta M^{\mathrm{self},t}$ the self-energy correction from (f), $\delta M^{v1,t}$ from (g) and (h), $\delta M^{v2,t}$ from (i) and (j), $\delta M^{\mathrm{box1},t}$ from (k), $\delta M^{\mathrm{box2},t}$ from (l) and $\delta M^{\mathrm{box3},t}$ from (m). In the following we only give the explicit results of the s channel (no crossed diagram) and t channel contributions. The u channel results can be obtained by the following substitutions:

$$p_3 \leftrightarrow p_4, \quad a \leftrightarrow b, \quad \hat{t} \leftrightarrow \hat{u}. \tag{20}$$

All s-, t-channel terms in δM^+, δM^-, δM^δ can be written as followed according to their Lorentz structures:

$$\begin{aligned}\delta M^X = \epsilon_4^\mu \epsilon_3^\nu \bar{u}_2 [& f_1^X g_{\mu\nu} + f_2^X \gamma_\mu \gamma_\nu + f_7^X p_{1\mu} p_{1\nu} + f_8^X p_{1\mu} p_{2\nu} \\ & + f_9^X p_{2\mu} p_{1\nu} + f_{10}^X p_{2\mu} p_{2\nu} + f_{13}^X \not{p}_4 p_{1\nu} \gamma_\mu + f_{14}^X \not{p}_4 p_{1\mu} \gamma_\nu \\ & + f_{15}^X \not{p}_4 p_{2\nu} \gamma_\mu + f_{16}^X \not{p}_4 p_{2\mu} \gamma_\nu] \gamma_5 v_1, \end{aligned} \tag{21}$$

where $X = s1,\ s2,\ \mathrm{self},\ v1,\ v2,\ \mathrm{box1},\ \mathrm{box2},\ \mathrm{box3}$, respectively. The ten form factors corresponding to each diagram are given in Appendix A. They are not all independent when we sum over all possible channels. CP-odd property of δM^X requires

$$f_{13}^X = f_{16}^X, \quad f_{14}^X = f_{15}^X, \quad f_7^X + 2f_{14}^X = f_{10}^X. \tag{22}$$

Those relations are verified by our explicit formula of the form factors. We find that all form factors are proportional to $\lambda_{CP} = 2\,\mathrm{Im}(a_1 b_1^\star) = \sin 2\theta_t \sin\beta_t$.

The color sum of the amplitude square including the next-to-leading order correction is

$$\begin{aligned}\sum_{\mathrm{color}} & \{|M_0^g|^2 + 2\,\mathrm{Re}(M_0^g \delta M^{gA\dagger})\} \\ & = g_s^4 \{\tfrac{7}{3}|M_0^+|^2 + 3|M_0^-|^2 + \tfrac{14}{3}\mathrm{Re}(M_0^+ \delta M^{+\dagger}) \\ & \quad + 6\,\mathrm{Re}(M_0^- \delta M^{-\dagger}) + 8\,\mathrm{Re}(M_0^+ \delta M^{\delta\dagger})\}, \end{aligned} \tag{23}$$

where

$$M_0^+ = M_0^t + M_0^u, \quad M_0^- = M_0^t - M_0^u - 2M_0^s. \tag{24}$$

B. *CP* violation in 2HDM

In ordinary 2HDM, there are three neutral physical Higgs bosons, namely, two CP-even scalars H, h, one CP-odd pseudoscalar A. CP violation in the scalar potential [22] induces mixing of the CP-even and CP-odd neutral Higgs bosons, thus leading to three physical mass eigenstates $|\phi_j\rangle (j=1,2,3)$ with no definite CP parity. Their Yukawa couplings to the top quark can be written as (in the notation of [23])

$$L_Y = -m_t(\sqrt{2}G_F)^{1/2} \sum_{j=1}^{3} \bar{t}(a_{jt} + i\tilde{a}_{jt}\gamma_5) t \phi_j, \tag{25}$$

where G_F is the Fermi constant, and

$$a_{jt} = d_{2j}/\sin\beta, \quad \tilde{a}_{jt} = -d_{3j}\cot\beta, \tag{26}$$

and d_{2j}, d_{3j} are the matrix elements of a 3×3 orthogonal matrix that describes the mixing of the neutral states [23]. We assume that the two heavier Higgs bosons ($j=2,3$) may be neglected and define $a = a_{1t}$, $\tilde{a} = \tilde{a}_{1t}$, $\phi = \phi_1$. The strength of CP violation is proportional to $2\,\mathrm{Im}[a_{1t}(-i\tilde{a}_{1t})^\star] = 2a\tilde{a} = -2\gamma_{CP}$ (γ_{CP} is defined in [12]).

The one-loop Feynman diagrams of Higgs boson contributions to the processes $q\bar{q}\to t\bar{t}$ and $gg\to t\bar{t}$ can be represented by Fig. 1(b) and Figs. 2(c), (f), (g), (i), (k), and (n), respectively. Now the dashed lines in the loop stand for Higgs bosons, while the solid lines for top quarks.

The one-loop amplitudes can be easily obtained from those of the MSSM by the method given in Appendix A with no changes on δM^{qv}, δM^+, δM^- and the modification on δM^δ which comes from Fig. 2(n):

$$\delta M^{\delta}=\epsilon_4^{\mu}\epsilon_3^{\nu}\bar{u}_2\{a^2(f_1^{sr}g_{\mu\nu}+f_2^{sr}p_{3\mu}p_{4\nu})-\tilde{a}^2 f_3^{sr} i\epsilon_{\mu\nu\rho\sigma}p_4^{\rho}p_3^{\sigma}\gamma_5$$
$$+a\tilde{a}[i(f_1^{sr}g_{\mu\nu}+f_2^{sr}p_{3\mu}p_{4\nu})\gamma_5$$
$$-f_3^{sr}\epsilon_{\mu\nu\rho\sigma}p_4^{\rho}p_3^{\sigma}]\}v_1/(\hat{s}-m_{\phi}^2+im_{\phi}\Gamma_{\phi}), \quad (27)$$

where Γ_{ϕ} is the Higgs boson width and $f_{1,2,3}^{sr}$ are given in Appendix A. δM^{δ} is composed of two parts: $\delta M^{\delta e}$, which is CP even and contains terms of a^2, $\tilde{a}^2$; $\delta M^{\delta o}$, the CP odd term proportional to $a\tilde{a}$. We keep the CP-even term because when $m_{\phi}>2m_t$, it may be important. The $8\mathrm{Re}(M_0^{+}\delta M^{\delta\dagger})$ term in the color sum of Eq. (23) should be replaced by

$$8\mathrm{Re}(M_0^{+}\delta M^{\delta\dagger})+24(|\delta M^{\delta e}|^2+|\delta M^{\delta o}|^2)$$
$$+48\mathrm{Re}(\delta M^{\delta e}\delta M^{\delta o\dagger}). \quad (28)$$

We compute Γ_{ϕ} by using the formula and parameters of Ref. [12].[1]

C. *CP* violation from model-independent top quark CEDM

When the particles in the loops are heavy compared to the external particle momenta, it is convenient to describe the loop induced interactions by an effective interaction Lagrangian. Even when the loop masses are not too large, a model-independent study can give us knowledge about the sensitivities of given colliders. That approach is particularly useful when we do not know the underlying new physics. We assume the following additional top-quark-gluon effective interaction

$$L_D=\frac{id_t}{2}\bar{t}\sigma^{\mu\nu}\gamma_5 F_{\mu\nu}^{a}T^{a}t, \quad (29)$$

where $\sigma^{\mu\nu}=(i/2)[\gamma^{\mu},\gamma^{\nu}]$, $F_{\mu\nu}^{a}$ is the the gluon field strength. The coefficient d_t is the top quark chromoelectric dipole moment (CEDM) which we assume to have an imaginary part as well as a real part. We denote it as $d_t^R+id_t^I$.

The CEDM d_t contributes to the CP-violating amplitudes through the diagrams of Fig. 3. Let us define $\hat{d}_t=d_t/g_s=\hat{d}_t^R+i\hat{d}_t^I$. The contribution of Fig. 3(a) to $q\bar{q}\to t\bar{t}$ can be obtained by simply replacing D^s with $i\hat{d}_t$ in Eq. (14) and setting $\delta M^{DB}=\delta M^{CB}=0$. We denote the contributions to $gg\to t\bar{t}$ of Figs. 3(b)–(e) as δM^s, δM^b, $\delta M^{v,t}$, $\delta M^{v,u}$ (for the crossed diagrams), respectively. Then we have

$$\delta M^{+}=\delta M^{v,t}+\delta M^{v,u},$$
$$\delta M^{-}=-2\,\delta M^{s}-2\,\delta M^{b}+\delta M^{v,t}-\delta M^{v,u},$$
$$\delta M^{\delta}=0. \quad (30)$$

δM^s, δM^b, $\delta M^{v,t}$ can also be written as the form of Eq. (21) with the constant form factors given in Appendix A.

[1]The misprint of Γ_Z is corrected.

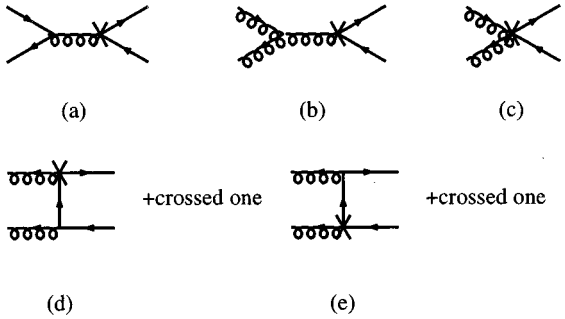

FIG. 3. Feynman diagrams of top quark CEDM corrections of CP violation to $q\bar{q}\to t\bar{t}$, $gg\to t\bar{t}$.

III. EXTRACTING THE *CP*-VIOLATING EFFECTS

Since δM^{aA} contains odd combinations of γ_5 and $\epsilon_{\mu\nu\rho\sigma}$, its interference with the tree-level amplitude will be zero if we sum up all the initial and final state spins or polarizations. To see the CP-violating effects, the spins of at least some of the particles must be identified. Because the initial state spins are difficult to determine, the helicities of the final $t\bar{t}$ must be inferred from their decays. If we assume the SM couplings of the top quark to its decay products and set $m_b=0$, all decay products of the top quark will have left-handed helicities. That means the spin information of the top quark can only be transfered to the momentum correlations among the decay products.

We assume the SM decay of the top quark[2] and apply the narrow width approximations of the top quark and W-boson propagators:

$$\frac{1}{|q_Y^2-m_Y^2+im_Y\Gamma_Y|^2}\to\frac{\pi}{m_Y\Gamma_Y}\delta(q_Y^2-m_Y^2), \quad (31)$$

where Y stands for top quark and W boson, Γ_Y is the width of Y.

The parton level cross section for reaction $a\bar{a}\to t\bar{t}\to bl_1^{+}\nu_{l_1}\bar{b}l_2^{-}\bar{\nu}_{l_2}$ $(b\bar{q}_1q_1'\bar{b}q_2\bar{q}_2')$ can be written as

$$d\hat{\sigma}_{a\bar{a}}=\frac{\gamma}{(8\pi)^{10}\hat{s}}\frac{\lambda_t\overline{|M|}_a^2}{m_t^2m_W^2\Gamma_t^2\Gamma_W^2}d\Omega_t d\Omega'_{W^+}d\Omega'_{W^-}d\Omega'_{l_1^+}d\Omega'_{l_2^-}, \quad (32)$$

where $\gamma=\sqrt{1-4m_t^2/\hat{s}}$ and

$$\lambda_t=\left[1-\frac{(m_W+m_b)^2}{m_t^2}\right]\left[1-\frac{(m_W-m_b)^2}{m_t^2}\right]\approx(m_t^2-m_W^2)^2/m_t^4, \quad (33)$$

$d\Omega'_{W^+}(d\Omega'_{W^-})$ is the solid angle element of $W^+(W^-)$ in the rest frame of the (anti) top quark, $d\Omega'_{l_1^+}(d\Omega'_{l_2^-})$ denotes the

[2]The top quark decay asymmetry in the MSSM is found to be small [16,24].

solid angle element of $l_1^+(l_2^-)$ in the rest frame of $W^+(W^-)$, $\overline{|M|}_a^2$ is the average amplitude square excluding the top quark and W-boson propagators after the decays of the top quarks:

$$\overline{|M|}_a^2 = S_a^{-1} \sum_{\text{color,spin}} \{|M_0^a|^2 + 2\text{Re}(M_0^a \delta M^{aA\dagger})\}, \quad (34)$$

where $1/S_a$ is the color,spin average factor: $S_q = 36$ and $S_g = 256$. In our calculations, $\overline{|M|}_a^2$ is easily obtained from the amplitude of $a\bar{a} \to t\bar{t}$ by the following substitutions:

$$\bar{u}_2 \to \frac{g^2}{8} \bar{u}_b \gamma_\mu (1-\gamma_5)(\not{p}_2 + m_t) \bar{u}_{\nu_1} \gamma^\mu (1-\gamma_5) v_{l_1},$$
$$v_1 \to \frac{g^2}{8} \bar{u}_{l_2} \gamma_\mu (1-\gamma_5) v_{\nu_2} (\not{p}_1 - m_t) \gamma^\mu (1-\gamma_5) v_{\bar{b}}, \quad (35)$$

where g is the weak SU(2) coupling constant. The above expresssions are calculated numerically.

The hadronic cross section is obtained by convoluting Eq. (32) with parton distribution functions:

$$d\sigma_{p\bar{p}(p)} = \sum_{a=q,g} \int_0^1 dx_1 \int_0^1 dx_2 [f_a^p(x_1) f_{\bar{a}}^{\bar{p}(p)}(x_2) + (p \leftrightarrow \bar{p}(p))] d\hat{\sigma}_{a\bar{a}} / (1 + \delta_{a,\bar{a}}), \quad (36)$$

where $f_a^{\bar{p}(p)}$, $f_{\bar{a}}^{\bar{p}(p)}$ are parton distribution functions (PDFs).

It has been studied extensively in the literature how to pick out the momentum correlation information contained in $2\text{Re}(M_0^a \delta M^{aA\dagger})$ and therefore the CP-violating effects by looking at the expectation values of the CP-odd observables constructed from the momenta of the top quarks and their decay products [5–12,16,25–28]. In this study, we adopt the following simple observables that are constructed from observed momenta and can be easily used by experimentalists:

$$A_1 = E_{l^+} - E_{l^-}, \quad (37)$$

$$A_2 = \vec{p}_{\bar{t}} \cdot \vec{p}_{l^+} - \vec{p}_t \cdot \vec{p}_{l^-} \equiv O_{\bar{t}} - Q_t, \quad (38)$$

$$T_2 = (\vec{p}_b - \vec{p}_{\bar{b}}) \cdot (\vec{p}_{l^+} \times \vec{p}_{l^-}), \quad (39)$$

$$f_2 = \frac{\epsilon_{\mu\nu\sigma\rho} p_{l^+}^\mu p_{l^-}^\nu p_b^\sigma p_{\bar{b}}^\rho}{(p_{l^+} \cdot p_{l^-} p_b \cdot p_{\bar{b}})^{1/2}}, \quad (40)$$

$$\hat{O}_L = \frac{1}{m_t^3 |\vec{P}|^2} \vec{P} \cdot (\vec{p}_{l^+} \times \vec{p}_{l^-}) \vec{P} \cdot (\vec{p}_{l^+} - \vec{p}_{l^-}), \quad (41)$$

where all momenta are in the laboratory frame, $E_{l^+}(E_{l^-})$ is the energy of $l^+(l^-)$ ($l = l_1 = l_2 = e,\ \mu$, here we do not distinguish $e,\ \mu$), the subscripts of the momenta denote the corresponding particles, $\vec{P}$ is the momentum of the proton in the case of $p\bar{p}$ collision. A_1, A_2, and T_2 are studied in Ref. [12]. f_2 and $\hat{O}_L$ are used in Refs. [8,11], respectively. Because A_1, A_2 are $\hat{T}$ (time reflection [27,29]) even, they are only sensitive to the absorptive parts (imaginary parts) of the loop calculations and $\hat{d}_t$. On the contrary, T_2, f_2, and $\hat{O}_L$ are $\hat{T}$ odd and only sensitive to the dispersive parts (real parts). A_1, T_2, f_2, and $\hat{O}_L$ all require the events that two top quarks decay semileptonically. A_2 uses the events that one top quark decays semileptonically and the other hadronically. Among the above observables, only f_2 is Lorentz invariant.

While all the above naive observables use only parts of the information, the optimal observables studied in Refs. [30–32] use the full information in $2\text{Re}(M_0^a \delta M^{aA\dagger})$. Therefore they are the most effective ones.

In the case of model-independent top quark CEDM, $2\text{Re}(M_0^a \delta M^{aA\dagger})$ contains two terms that are proportional to $\hat{d}_t^R$ and $\hat{d}_t^I$, respectively. In the MSSM , it depends on the particle masses in the loop as well as a multiplicative constant λ_{CP}. However, since our main goal is to search for CP violation induced by this λ_{CP}, we must assume all the masses in the loop are known. In the 2HDM, from the first term in Eq. (28) which is CP odd, one can separate a factor $\gamma_{CP} = -a\tilde{a}$. Although in the resonant region, contributions of the other three terms (belonging to higher than next-to-leading order) may be large, they are still overwhelmed by the tree-level and the next-to-leading order contributions. As an approximation, we shall drop them in the definitions of the optimal observables. Therefore we can always separate a constant (denote it as $\lambda = \lambda_{CP}$, γ_{CP}, $\hat{d}_t^R$, $\hat{d}_t^I$) from $2\text{Re}(M_0^a \delta M^{aA\dagger})$ in all the models considered.

Apart from some common factors in Eq. (36), the hadronic cross section can be written as

$$d\sigma_{p\bar{p}(p)} = \sum_{a=q,g} \int \sum_{\text{color,spin}} \{|M_0^a|^2 + \lambda 2\text{Re}(M_0^a \delta M^{aA\dagger})\} \times [f_a^p(x_1) f_{\bar{a}}^{\bar{p}(p)}(x_2) + (p \leftrightarrow \bar{p}(p))] d\Phi\ dx_1 dx_2, \quad (42)$$

where $d\Phi$ denotes the phase space. In the following, $2\text{Re}(M_0^a \delta M^{aA\dagger})$ is calculated by setting $\lambda_{CP} = 1$, $\gamma_{CP} = 1$, $\hat{d}_t = 1$, and $\hat{d}_t = i$ in the form factors in each model, respectively. The optimal observable is defined as

$$O_{opt} = \frac{\sum_{a=q,g} \sum_{\text{color,spin}} 2\text{Re}(M_0^a \delta M^{aA\dagger})[f_a^p(x_1) f_{\bar{a}}^{\bar{p}(p)}(x_2) + (p \leftrightarrow \bar{p}(p))]}{\sum_{a=q,g} \sum_{\text{color,spin}} |M_0^a|^2 [f_a^p(x_1) f_{\bar{a}}^{\bar{p}(p)}(x_2) + (p \leftrightarrow \bar{p}(p))]}. \quad (43)$$

The above observable depends on the parton distribution functions. It is inconvenient for practical use. In the pp collision, it is not a CP-odd observable because of the asymmetry of quark PDFs (cf. Appendix C). Because at the 2 TeV Fermilab Tevatron, the main $t\bar{t}$ production mechanism is $q\bar{q}\to t\bar{t}$, and at the 14 TeV CERN LHC, the main process is $gg\to t\bar{t}$, we can neglect one process at each collider. We consider only $q\bar{q}\to t\bar{t}$ at the Fermilab Tevatron and $gg\to t\bar{t}$ at the CERN LHC in all of the following calculations. Then we have the optimal observable

$$O_1=\frac{\sum_{\text{color,spin}} 2\text{Re}(M_0^a \delta M^{aA\dagger})}{\sum_{\text{color,spin}} |M_0^a|^2}. \tag{44}$$

Since the neglected process consists of only about 10% of the total cross section, Eq. (44) deviates from the truly optimal observable by at most 20%. O_1 has the property of Lorentz invariance, one can calculate it in any frame. It has the same symmetry property as $2\text{Re}(M_0^a \delta M^{aA\dagger})$ which is CP odd. In the MSSM and 2HDM, O_1 has no definite $\hat{T}$ parity and depends on the loop particle masses. We note that the optimal observable defined for $\hat{d}_t^R$ is only sensitive to $\hat{d}_t^R$ independent of $\hat{d}_t^I$. The same holds true for $\hat{d}_t^I$. This is because the two terms proportional to d_t^R and d_t^I have different discrete symmetry $\hat{T}$.

To calculate O_1, we need to know all the momenta of the initial and final state particles. That cannot always be achieved. It is still useful because it can provide us with the upper limit signal to noise ratios of any other CP-odd observables. Let us first look at the case where two top quarks decay semileptonically. The two neutrino momenta p_{ν_1}, p_{ν_2} will be unknown. But they may be determined indirectly by the following eight equations [8]:

$$p_{\nu_1}^2=p_{\nu_2}^2=0,$$

$$(p_{\nu_1}+p_{l_1^+})^2=(p_{\nu_2}+p_{l_2^-})^2=m_W^2, \tag{45}$$

$$(p_{\nu_1}+p_{l_1^+}+p_b)^2=m_t^2,$$

$$(p_{\nu_2}+p_{l_2^-}+p_{\bar{b}})^2=m_t^2,$$

$$(p_{\nu_2}+p_{l_2^-}+p_{\bar{b}})_{\text{transverse}}=-(p_{\nu_1}+p_{l_1^+}+p_b)_{\text{transverse}}.$$

Similar situation exists in the study of $\tau\bar{\tau}$ production in e^+e^- collision [33]. The above equations give rise up to fourfold solutions (see Appendix B). Considering this ambiguity, we can define a modified optimal observable

$$O_l=\frac{\sum_{\text{color,spin},i} 2\text{Re}(M_0^a \delta M^{aA\dagger})\,\eta_i}{\sum_{\text{color,spin},i} |M_0^a|^2\,\eta_i}, \tag{46}$$

where the sum i is over all possible solutions of the neutrino momenta $\eta_i=\gamma_i/\hat{s}_i[f_a^p(x_1^i)f_{\bar{a}}^{\bar{p}(\bar{p})}(x_2^i)+(p\leftrightarrow p(\bar{p}))]$ comes from the $t\bar{t}$ phase space, flux factor, and PDFs because of different momentum reconstruction [cf. Eqs.(32) and (36)]. There may be possibility that the reconstructed initial parton energy exceeds the proton(antiproton) energy. That kind of reconstruction should be discarded in the calculations. O_l also depends on PDFs. For practical use, we define a nonoptimal observable as an approximation:

$$O_l'=\sum_i O_1. \tag{47}$$

Again the sum i is over all possible solutions of the neutrino momentum.[3]

We now consider the case where one top quark decays semileptonically and the other hadronically. The missing neutrino momentum can be fully reconstructed [34]. But because we cannot distinguish the quark and antiquark jet, we still have ambiguity of twofold uncertainty. When two quarks decay all hadronically, there is fourfold uncertainty. We define therefore alternatvely the optimal observables

$$O_2=\frac{\sum_{\text{color,spin},j} 2\text{Re}(M_0^a \delta M^{aA\dagger})}{\sum_{\text{color,spin},j} |M_0^a|^2}, \tag{48}$$

$$O_4=\frac{\sum_{\text{color,spin},j'} 2\text{Re}(M_0^a \delta M^{aA\dagger})}{\sum_{\text{color,spin},j'} |M_0^a|^2}, \tag{49}$$

where the sum j in O_2 is over the two possible assignments of the jet momenta, and the sum j' in O_4 is over the four assignments.

The statistical significance of an observable O can be described by the signal to noise ratio r defined as

$$r=\langle O\rangle/\sqrt{\langle O^2\rangle}, \tag{50}$$

where $\langle O\rangle,\langle O^2\rangle$ are the expectation value of O, O^2, respectively:

[3]One can also define O_l' by setting $\eta_i=1$ in Eq. (46), the numerical difference between the two definitions is minor.

$$\langle O^n\rangle = \frac{\int O^n d\sigma_{p\bar{p}(p)}}{\int d\sigma_{p\bar{p}(p)}}. \tag{51}$$

It is interesting to note that for the optimal observables and unit λ, we always have $\langle O\rangle = \langle O^2\rangle$. Care must be taken in calculating the r of A_2. Because A_2 is the difference of two observables ($O_{\bar{t}}$ and O_t) which are calculated using different events (i.e., different independent distribution functions), we have $\langle A_2^2\rangle = \langle O_t^2\rangle + \langle O_t^2\rangle \approx 2\langle O_t^2\rangle$. If the experimental error comes only from statistics, the number of events N_{event} needed to observe CP violating effects at 1σ level (68% C.L.) satisfies $|r| \geqslant 1/\sqrt{N_{\text{event}}}$ or $N_{\text{event}} \geqslant 1/r^2$. To reduce the statistical errors, one can combine the measured results of the three decay modes: leptonic-leptonic, leptonic-hadronic, and hadronic-hadronic modes [15]. Assuming their corresponding number of events are N_{ll}, N_{jl} and N_{jj}, respectively, then we can define a combined signal to noise ratio:

$$r_c = \sqrt{(N_{ll} r_1^2 + N_{jl} r_2^2 + N_{jj} r_3^2)/N}, \tag{52}$$

where r_1, r_2, and r_3 are the signal to noise ratios of the observables which use leptonic-leptonic, leptonic-hadronic, and hadronic-hadronic events, respectively. $N = N_{ll} + N_{jl} + N_{jj}$ is the total number of events of the three modes. Note that r_c depends only on the ratios N_{ll}/N, N_{jl}/N, and N_{jj}/N, not on N. The signal is detectable at 1σ level when $|r_c| \geqslant 1/\sqrt{N}$.

IV. NUMERICAL RESULTS AND CONCLUSIONS

We first check our calculations with QCD gauge invariance in the process $gg \to t\bar{t}$. That can be done by replacing ϵ_3, ϵ_4 with p_3, p_4. We find that the correction amplitude is consistent with gauge invariance. Then we check our calculations with known results in the literature. Our parton level results are all in agreement with Refs. [7,12]. By using $\sqrt{s} = 40$ TeV, $m_t = 160$ GeV, and 10^7 sample of leptonic events, we find the O_1 limit on d_t^R is 2.8×10^{-20} cm g_s which is very close to $\lambda_{\min}$ in Ref. [8]. That means that taking the top quark spin in its rest frame to be in the direction of lepton momentum is feasible. We can also reproduce the results of $\hat{O}_L$ in Ref. [11] with $\mu_t' = 0$ by including both $q\bar{q} \to t\bar{t}$ and $gg \to t\bar{t}$ processes in the calculations.

As mentioned previously, in the following calculations, we consider only $q\bar{q} \to t\bar{t}$ at the Fermilab Tevatron and $gg \to t\bar{t}$ at the CERN LHC. The parton distribution functions of Martin-Roberts-Stirling (MRS) set A' [35] with scale $Q^2 = m_t^2$ are used.[4] m_t is taken to be 176 GeV. To look at the largest possible effects, we set the CP-violating parameters λ_{CP} and γ_{CP} to be of order 1, namely, $\lambda_{CP} = 1$ (this needs $\theta_t = \pi/4$, cf. Appendix A), $\gamma_{CP} = 1$. In the MSSM and 2HDM, we treat the SUSY particle masses and Higgs boson mass as free parameters allowed by current experiments. We assume that all the squarks except for the light top squark $\tilde{t}_1$ to be degenerate. The light top mass is required to be above 50 GeV [37]. We choose gluino mass $m_{\tilde{g}}$ and Higgs boson mass $\geqslant 100$ GeV.

The signal to noise ratio results at the 2 TeV $p\bar{p}$ Fermilab Tevatron and at the 14 TeV pp CERN LHC are summarized in Tables I–V. We do not present the results for 2HDM at the Fermilab Tevatron because the effects are too small unless the Higgs boson mass is less than 100 GeV. We denote the signal to noise ratio r of an observable O as $r(O)$. All the tables show that $r(O_l')$ is slightly smaller than $r(O_1)$ and $r(O_2)$ is about 3/4 of $r(O_1)$, $r(O_4)$ about 1/2 of $r(O_1)$. Therefore, O_l' is a good approximation for O_1.

Table I shows the results at the Fermilab Tevatron from five sets of SUSY parameters. We see that the naive observables have signal to noise ratios all $\leqslant 1\%$. It is difficult to observe such small effects at the Fermilab Tevatron. The optimal observables, on the other hand, have $r \geqslant 1\%$ as long as the gluino mass is around 200 GeV.[5] They are about 3–10 times more effective than the naive ones. The combined signal to noise ratios of O_l', O_2, and O_4 are all between these of O_2 and O_4. Because N_{ll} is small compared with N_{jl} and N_{jj}, the combined r is just a weighted average of these of O_2 and O_4. Assuming we can obtain 30 fb^{-1} integrated luminosity, then the total number of fully reconstructed $t\bar{t}$ events is about 3.5×10^4 [1]. It is reasonable to assume that we can have purely hadronic events $N_{jj} = 2 \times 10^4$, hadronic-leptonic events $N_{jl} = 1.2 \times 10^4$, and purely leptonic events $N_{ll} = 0.2 \times 10^4$. The corresponding 1 σ level statistical errors are $r_{jj} = 0.71 \times 10^{-2}$, $r_{jl} = 0.91 \times 10^{-2}$, $r_{ll} = 2.2 \times 10^{-2}$. The combined error is 0.54%. In Table I, O_l' has $r > r_{ll}$ only when $m_{\tilde{t}_1}$ is around 50 GeV and $m_{\tilde{g}}$ is around 200 GeV. We always have $r(O_2) > r_{jl}$, $r(O_4) > r_{jj}$ when $m_{\tilde{g}} \sim 200$ GeV. Therefore, it is possible to detect the CP-violating effects by using optimal observables O_2 and O_4 when $m_{\tilde{g}}$ is around 200 GeV. The effects are detectable by a combined measurement when $m_{\tilde{g}}$ is in the range 100–300 GeV.

Table II shows the results at the CERN LHC in MSSM. It shows the same features as Table I. However, at the CERN LHC, the numbers of events are much larger than those at the Fermilab Tevatron. With 150 fb^{-1} integrated luminosity, we can assume $N_{jj} = 10^7$, $N_{jl} = 6 \times 10^6$, and $N_{ll} = 10^6$. We further assume the experimental systematic errors are below the statistical ones. In addition, there are also theoretical uncertainties coming from possible non-CP-violating contaminations at the pp CERN LHC. Because the initial pp state is not a CP eigenstate, CP-conserving interactions can produce CP-asymmetry effects in $t\bar{t}$ final state. We present a general analysis of the contaminations to the Lorentz invariant observables in Appendix C. We find that within the

[4] It should be noted that all the results are insensitive to the PDF and Q^2 choices. CTEQ4M [36] gives similar results.

[5] The value is close to m_t, so that the gluino threshold is close to the top quark one. The CP-violating effects are large because of the threshold effects.

TABLE I. Signal to noise ratio r in $p\bar{p}\to t\bar{t}+X$ at the 2 TeV Fermilab Tevatron in the MSSM with $\lambda_{CP}=1$, for five sets of SUSY parameters labeled by $(m_{\tilde{t}_1}, m_{\tilde{t}_2}=m_{\tilde{q}}, m_{\tilde{g}})$ GeV. The combined results are for O_l', O_2, and O_4.

	A_1	A_2	T_2	f_2	O_1	O_l'	O_2	O_4	Combined
(100,500,100)	0.25%	−0.23%	−0.16%	−0.16%	0.82%	0.79%	0.62%	0.45%	0.54%
(100,500,200)	0.59%	−0.42%	0.08%	0.12%	1.82%	1.73%	1.41%	1.04%	1.18%
(100,500,300)	0.12%	−0.17%	0.13%	0.11%	0.78%	0.74%	0.56%	0.40%	0.49%
(50,500,200)	0.80%	−0.58%	0.08%	0.14%	2.49%	2.37%	1.93%	1.43%	1.69%
(100,1000,200)	0.58%	−0.42%	0.11%	0.15%	1.77%	1.68%	1.36%	1.01%	1.19%

TABLE II. Signal to noise ratio r in $pp\to t\bar{t}+X$ at the CERN LHC in the MSSM with $\lambda_{CP}=1$, for six sets of SUSY parameters labeled by $(m_{\tilde{t}_1}, m_{\tilde{t}_2}, m_{\tilde{g}})$ GeV. The combined results are for O_l', O_2, and O_4.

	A_1	T_2	f_2	O_1	O_l'	O_2	O_4	Combined
(100,500,100)	−0.12%	0.11%	0.22%	0.92%	0.81%	0.71%	0.53%	0.62%
(100,500,200)	0.41%	−0.13%	−0.35%	1.82%	1.61%	1.41%	1.05%	1.23%
(100,500,300)	0.17%	−0.13%	−0.29%	0.85%	0.72%	0.62%	0.44%	0.53%
(100,500,400)	0.06%	−0.08%	−0.17%	0.41%	0.34%	0.29%	0.20%	0.24%
(50,500,200)	0.63%	−0.14%	−0.42%	2.50%	2.22%	1.97%	1.47%	1.71%
(100,1000,200)	0.47%	−0.17%	−0.48%	2.12%	1.88%	1.62%	1.20%	1.41%

TABLE III. Signal to noise ratio r in $pp\to t\bar{t}+X$ at the CERN LHC in the 2HDM with $\gamma_{CP}=1$. The combined results are for O_l', O_2, and O_4.

m_ϕ(GeV)	A_1	T_2	f_2	O_1	O_l'	O_2	O_4	Combined
100	−0.20%	0.10%	0.28%	1.09%	0.97%	0.82%	0.60%	0.71%
200	−0.16%	0.12%	0.30%	0.96%	0.85%	0.69%	0.49%	0.59%
300	−0.15%	0.14%	0.36%	1.12%	0.97%	0.78%	0.54%	0.66%
400	−0.13%	0.20%	0.45%	1.55%	1.52%	1.31%	0.92%	1.11%
500	−0.05%	0.15%	0.31%	0.91%	0.87%	0.76%	0.53%	0.64%

TABLE IV. Signal to noise ratio r at the Fermilab Tevatron and CERN LHC with model independent top quark CEDM $d_t^R=1$ GeV^{-1} $g_s=1.97\times10^{-14}$ cm g_s, and the accuracies with which d_t^R can be measured at the Fermilab Tevatron and CERN LHC with assumed numbers of events given in the text. d_t^R is given in units of 10^{-18} cm g_s. O_1 is given only for leptonic events. The combined results are for O_l', O_2, O_4.

		T_2	f_2	$\hat{O}_L$	O_1	O_l'	O_2	O_4	Combined
Tevatron	r	39.9	40.9	−35.2	124	88	75	47	61
	d_t^R	10.9	10.6	12.3	3.5	4.9	2.4	3.0	1.7
LHC	r	−53.6	−112		238	199	154	99	128
	d_t^R	0.37	0.18		0.08	0.10	0.052	0.064	0.037

TABLE V. The same as Table IV, but for d_t^I.

		A_1	A_2	O_1	O_l'	O_2	O_4	Combined
Tevatron	r	−80.5	57.4	214	179	169	127	146
	d_t^I	5.4	4.4[a]	2.0	2.4	1.1	1.1	0.73
LHC	r	83.2	−21.1	381	332	332	248	282
	d_t^I	0.24	5.8 [a]	0.052	0.059	0.025	0.025	0.017

[a]Note that for A_2, only half of N_{jl} can be used.

framework of a parton model, there are no contaminations to these observables. A_1, A_2, and T_2 are discussed in Refs. [6,12]. They are well below the signals. Therefore, the 1 σ level errors are $r_{jj}=0.32\times10^{-3}$, $r_{jl}=0.41\times10^{-3}$, $r_{ll}=1.0\times10^{-3}$. The combined error is 0.24×10^{-3}. The naive observable T_2 is on the margin to be detectable. A_1 and f_2 are better than T_2. They can be used to observe λ_{CP} at few $\times10^{-1}$ when $m_{\tilde{g}}$ is within the range 100–400 GeV. The observable O_l' is 2–5 times better. All $r(O_2)\geqslant10$ r_{jl} and $r(O_4)\geqslant10$ r_{jj} for $m_{\tilde{g}}\sim$100–300 GeV. We can pin down λ_{CP} to 10^{-1} by using these optimal observables.

In Table III, we give the results of signal to noise ratios in 2HDM at the CERN LHC. It is obvious that A_1 and T_2 are only detectable and cannot be used to put limit on γ_{CP}. f_2 is 2 times better which may be used to limit γ_{CP} to $(3–4)\times10^{-1}$. All the optimal observables have r larger than about 10 times statistical errors. Therefore, they will put a limit of order 10^{-1} on γ_{CP}.

Tables IV and V are the results of model-independent top quark CEDM. An overall feature of the two tables is that both at Fermilab Tevatron and CERN LHC, the accuracies of d_t^I are better than those of d_t^R. With the above assumed numbers of events at the Fermilab Tevatron, the best limits on d_t^R and d_t^I are 2.4×10^{-18} cm g_s and 1.1×10^{-18} cm g_s, respectively, by using O_2. Also by using O_2 at the CERN LHC, we can obtain the limits of 5.2×10^{-20} cm g_s and 2.5×10^{-20} cm g_s on d_t^R and d_t^I, respectively.

To summarize, we have studied CP-violating effects in top quark pair production at the future 2 TeV $p\bar{p}$ Fermilab Tevatron and 14 TeV pp CERN LHC colliders. Three kinds of CP-violating sources, the SUSY CP-odd phase of the top squark trilinear soft breaking term, arg(A_t), the CP-odd parameter in 2HDM, and the model-independent top quark CEDM are investigated. Optimal observables as well as simple observables are used. The optimal obervables are usually 2–10 times more effective than the naive ones. It is possible to observe CP-violating effects from arg(A_t) in top quark pair production at the 2 TeV Fermilab Tevatron with ~30 fb^{-1} integrated luminosity when $m_{\tilde{g}}\sim200$ GeV. If a combined measurement is applied, the range of gluino mass in which the CP violating effects are detectable is $\sim$100–300 GeV. The CERN LHC with 150 fb^{-1} can put a limit of order 10^{-1} on λ_{CP} [therefore on arg(A_t)] in MSSM and γ_{CP} in 2HDM by using optimal observables provided the experimental errors are sufficiently small. The CEDM of the top quark can be measured to an accuracy of 10^{-18} cm g_s at the Fermilab Tevatron and few $\times10^{-20}$ cm g_s at the CERN LHC. More accurate measurement on d_t^I can be obtained than on d_t^R with given number of events.

ACKNOWLEDGMENTS

The author is grateful to O. Nachtmann and A. Brandenburg for helpful suggestions and discussions and to O. Nachtmann for carefully reading the manuscript. The author also benefits from communications with W. Hollik. This work was financially supported by the AvH Foundation of Germany.

APPENDIX A: FORM FACTORS

We give here the nonzero form factors for the matrix elements appearing in the text. They are written in terms of the conventional one-, two-, three-, and four-point scalar loop integrals defined in Ref. [38].

In the following, the form factors are given in the MSSM:

$$D^s=\sum_{j=1,2}\{F_1C_{11}(-p_2,k,m_{\tilde{t}_j},m_{\tilde{g}},m_{\tilde{g}})+F_2(C_0+C_{11})(-p_2,k,m_{\tilde{g}},m_{\tilde{t}_j},m_{\tilde{t}_j})\}\frac{\alpha_s}{4\pi}m_{\tilde{g}}(-1)^{j+1}i\lambda_{CP}, \tag{A1}$$

$$f^{DB}=\sum_{j=1,2}\{D_{13}(-p_2,p_4,p_3,m_{\tilde{t}_j},m_{\tilde{g}},m_{\tilde{q}},m_{\tilde{g}})\}\frac{\alpha_s}{4\pi}m_{\tilde{g}}(-1)^{j+1}i\lambda_{CP}, \tag{A2}$$

$$f_1^{s1}=-2D^s(p_1\cdot p_4-p_2\cdot p_4)/\hat{s}, \tag{A3}$$

$$f_8^{s1}=4D^s/\hat{s}, \tag{A4}$$

$$f_9^{s1}=-4D^s/\hat{s}. \tag{A5}$$

$$f_1^{s2}=\sum_{j=1,2}\{C_0(-p_2,k,m_{\tilde{g}},m_{\tilde{t}_j},m_{\tilde{t}_j})\}\frac{\alpha_s}{4\pi}m_{\tilde{g}}(-1)^{j+1}i\lambda_{CP}, \tag{A6}$$

$$f_2^{\text{self},t}=\sum_{j=1,2}\{-B_0(\hat{t},m_{\tilde{g}}^2,m_{\tilde{t}_j}^2)+B_0(m_t^2,m_{\tilde{g}}^2,m_{\tilde{t}_j}^2)\}\frac{(F_1+F_2)\alpha_s}{4\pi}m_{\tilde{g}}(-1)^{j+1}i\lambda_{CP}/(\hat{t}-m_t^2). \tag{A7}$$

$$f_2^{v1,t}=\sum_{j=1,2}\{-C_0(-p_2,p_4,m_{\tilde{t}_j},m_{\tilde{g}},m_{\tilde{g}})\}\frac{F_1\alpha_s}{4\pi}m_{\tilde{g}}(-1)^{j+1}i\lambda_{CP}, \tag{A8}$$

$$f_{16}^{v1,t}=2D^{v}/(\hat{t}-m_t^2).$$

$$f_{2}^{v2,t}=\sum_{j=1,2}\{-C_0(p_1,-p_3,m_{\tilde{t}_j},m_{\tilde{g}},m_{\tilde{g}})\}\frac{F_1\alpha_s}{4\pi}m_{\tilde{g}}(-1)^{j+1}i\lambda_{CP}, \tag{A9}$$

$$f_{9}^{v2,t}=4D^{v}/(\hat{t}-m_t^2), \tag{A10}$$

$$f_{13}^{v2,t}=2D^{v}/(\hat{t}-m_t^2), \tag{A11}$$

where

$$D^{v}=\sum_{j=1,2}\{F_1C_{11}(-p_2,p_4,m_{\tilde{t}_j},m_{\tilde{g}},m_{\tilde{g}}),+F_2(C_0+C_{11})(-p_2,p_4,m_{\tilde{g}},m_{\tilde{t}_j}m_{\tilde{t}_j})\}\frac{\alpha_s}{4\pi}m_{\tilde{g}}(-1)^{j+1}i\lambda_{CP}, \tag{A12}$$

$$f_{1}^{\mathrm{box1},t}=\sum_{j=1,2}\{-4D_{27}\}\frac{\alpha_s}{4\pi}m_{\tilde{g}}(-1)^{j+1}i\lambda_{CP}F_1, \tag{A13}$$

$$f_{2}^{\mathrm{box1},t}=\sum_{j=1,2}\{m_t^2(D_0+2D_{12}+2D_{13}+D_{24}+D_{25})-m_{\tilde{g}}^2D_0-2p_2\cdot p_4(2D_{12}+D_{24}-D_{26})$$

$$-2p_1\cdot p_4(D_{25}-D_{26})+4D_{27}\}\frac{\alpha_s}{4\pi}m_{\tilde{g}}(-1)^{j+1}i\lambda_{CP}F_1, \tag{A14}$$

$$f_{7}^{\mathrm{box1},t}=\sum_{j=1,2}\{-4D_{26}\}\frac{\alpha_s}{4\pi}m_{\tilde{g}}(-1)^{j+1}i\lambda_{CP}F_1, \tag{A15}$$

$$f_{8}^{\mathrm{box1},t}=\sum_{j=1,2}\{4(D_{25}-D_{26})\}\frac{\alpha_s}{4\pi}m_{\tilde{g}}(-1)^{j+1}i\lambda_{CP}F_1, \tag{A16}$$

$$f_{9}^{\mathrm{box1},t}=\sum_{j=1,2}\{4(D_{12}+D_{24}-D_{26})\}\frac{\alpha_s}{4\pi}m_{\tilde{g}}(-1)^{j+1}i\lambda_{CP}F_1, \tag{A17}$$

$$f_{10}^{\mathrm{box1},t}=\sum_{j=1,2}\{-4(D_{13}+D_{26})\}\frac{\alpha_s}{4\pi}m_{\tilde{g}}(-1)^{j+1}i\lambda_{CP}F_1, \tag{A18}$$

$$f_{13}^{\mathrm{box1},t}=\sum_{j=1,2}\{2D_{12}\}\frac{\alpha_s}{4\pi}m_{\tilde{g}}(-1)^{j+1}i\lambda_{CP}F_1, \tag{A19}$$

$$f_{14}^{\mathrm{box1},t}=\sum_{j=1,2}\{-2D_{13}\}\frac{\alpha_s}{4\pi}m_{\tilde{g}}(-1)^{j+1}i\lambda_{CP}F_1, \tag{A20}$$

$$f_{15}^{\mathrm{box1},t}=\sum_{j=1,2}\{-2D_{13}\}\frac{\alpha_s}{4\pi}m_{\tilde{g}}(-1)^{j+1}i\lambda_{CP}F_1, \tag{A21}$$

$$f_{16}^{\mathrm{box1},t}=\sum_{j=1,2}\{2D_{12}\}\frac{\alpha_s}{4\pi}m_{\tilde{g}}(-1)^{j+1}i\lambda_{CP}F_1. \tag{A22}$$

The above D functions have the arguments $(-p_2,p_4,p_3,m_{\tilde{t}_j},m_{\tilde{g}},m_{\tilde{g}},m_{\tilde{g}})$.

$$f_{1}^{\mathrm{box2},t}=\sum_{j=1,2}\{-4D_{27}\}\frac{\alpha_s}{4\pi}m_{\tilde{g}}(-1)^{j+1}i\lambda_{CP}F_2, \tag{A23}$$

$$f_{7}^{\mathrm{box2},t}=\sum_{j=1,2}\{-4(D_{13}+D_{26})\}\frac{\alpha_s}{4\pi}m_{\tilde{g}}(-1)^{j+1}i\lambda_{CP}F_2, \tag{A24}$$

$$f_8^{\mathrm{box2},t}=\sum_{j=1,2}\{4(D_{25}-D_{26})\}\frac{\alpha_s}{4\pi}m_{\tilde{g}}(-1)^{j+1}i\lambda_{CP}F_2, \tag{A25}$$

$$f_9^{\mathrm{box2},t}=\sum_{j=1,2}\{4(D_0+2D_{12}+D_{24}-D_{26})\}\frac{\alpha_s}{4\pi}m_{\tilde{g}}(-1)^{j+1}i\lambda_{CP}F_2, \tag{A26}$$

$$f_{10}^{\mathrm{box2},t}=\sum_{j=1,2}\{-4(D_{13}+D_{26})\}\frac{\alpha_s}{4\pi}m_{\tilde{g}}(-1)^{j+1}i\lambda_{CP}F_2. \tag{A27}$$

The above D functions have the arguments $(-p_2,p_4,p_3,m_{\tilde{g}},m_{\tilde{t}_j},m_{\tilde{t}_j},m_{\tilde{t}_j})$.

$$f_1^{\mathrm{box3},t}=\sum_{j=1,2}\{-4D_{27}\}\frac{\alpha_s}{4\pi}m_{\tilde{g}}(-1)^{j+1}i\lambda_{CP}F_1F_2, \tag{A28}$$

$$f_7^{\mathrm{box3},t}=\sum_{j=1,2}\{4(-D_{23}+D_{26})\}\frac{\alpha_s}{4\pi}m_{\tilde{g}}(-1)^{j+1}i\lambda_{CP}F_1F_2, \tag{A29}$$

$$f_8^{\mathrm{box3},t}=\sum_{j=1,2}\{4(-D_{25}+D_{26})\}\frac{\alpha_s}{4\pi}m_{\tilde{g}}(-1)^{j+1}i\lambda_{CP}F_1F_2, \tag{A30}$$

$$f_9^{\mathrm{box3},t}=\sum_{j=1,2}\{4(D_{12}-D_{13}+D_{24}-D_{25})\}\frac{\alpha_s}{4\pi}m_{\tilde{g}}(-1)^{j+1}i\lambda_{CP}F_1F_2, \tag{A31}$$

$$f_{10}^{\mathrm{box3},t}=\sum_{j=1,2}\{-4(D_{11}-D_{12}+D_{21}-D_{24})\}\frac{\alpha_s}{4\pi}m_{\tilde{g}}(-1)^{j+1}i\lambda_{CP}F_1F_2, \tag{A32}$$

$$f_{13}^{\mathrm{box3},t}=\sum_{j=1,2}\{2(D_{12}-D_{13})\}\frac{\alpha_s}{4\pi}m_{\tilde{g}}(-1)^{j+1}i\lambda_{CP}F_1F_2, \tag{A33}$$

$$f_{15}^{\mathrm{box3},t}=\sum_{j=1,2}\{-2(D_{11}-D_{12})\}\frac{\alpha_s}{4\pi}m_{\tilde{g}}(-1)^{j+1}i\lambda_{CP}F_1F_2. \tag{A34}$$

The above D functions have the arguments $(-p_2,p_4,-p_1,m_{\tilde{t}_j},m_{\tilde{g}},m_{\tilde{g}},m_{\tilde{t}_j})$.

In the above, the color factors $F_1=\frac{3}{2}$, $F_2=-\frac{1}{6}$, and $\lambda_{CP}=2\mathrm{Im}(a_1b_1^{\star})=\sin 2\theta_t\sin\beta_t$.

The form factors of 2HDM can be obtained from those of MSSM by setting $j=1$, $F_1=1$, $F_2=0$, $f^{DB}=f_n^{s2}=0$, and the following substitutions:

$$\lambda_{CP}\rightarrow 2a\tilde{a}=-2\gamma_{CP}, \tag{A35}$$

$$m_{\tilde{g}}\rightarrow m_t, \quad m_{\tilde{t}_1}\rightarrow m_{\phi_1}, \tag{A36}$$

$$\frac{\alpha_s}{4\pi}\rightarrow\frac{\sqrt{2}m_t^2G_F}{16\pi^2}. \tag{A37}$$

In 2HDM, the form factors of Fig. 2(n) defined in Eq. (27) are

$$f_1^{sr}=\frac{\sqrt{2}m_t^2G_F}{16\pi^2}\{4m_t[m_t^2C_0-p_3\cdot p_4(2C_{22}-2C_{23}+C_0)+\tfrac{1}{2}]\}, \tag{A38}$$

$$f_2^{sr}=\frac{\sqrt{2}m_t^2G_F}{16\pi^2}\{4m_t[C_0+4(C_{22}-C_{23})]\}, \tag{A39}$$

$$f_3^{sr}=\frac{\sqrt{2}m_t^2G_F}{16\pi^2}\{4m_tC_0\}, \tag{A40}$$

where the C function arguments are $(p_4,-k,m_t,m_t,m_t)$.

The constant model-independent form factors are

$$D^s = i\hat{d}_t, \tag{A41}$$

$$f_1^s = -2i\hat{d}_t(p_1\cdot p_4 - p_2\cdot p_4)/\hat{s}, \tag{A42}$$

$$f_8^s = 4i\hat{d}_t/\hat{s}, \tag{A43}$$

$$f_9^s = -4i\hat{d}_t/\hat{s}, \tag{A44}$$

$$f_2^{v,t} = 2i\hat{d}_t, \tag{A45}$$

$$f_9^{v,t} = 4i\hat{d}_t/(\hat{t}-m_t^2), \tag{A46}$$

$$f_{13}^{v,t} = 2i\hat{d}_t/(\hat{t}-m_t^2), \tag{A47}$$

$$f_{16}^{v,t} = 2i\hat{d}_t/(\hat{t}-m_t^2), \tag{A48}$$

$$f_1^b = -i\hat{d}_t, \tag{A49}$$

$$f_2^b = i\hat{d}_t, \tag{A50}$$

where $\hat{d}_t$ is defined in the text.

Other definitions are

$$k = p_1+p_2 = p_3+p_4, \quad \hat{s} = k^2, \quad \hat{t} = q^2 = (p_2-p_4)^2,$$
$$\hat{u} = (p_2-p_3)^2, \tag{A51}$$

$$\Gamma^\mu = (-p_4+p_3)^\mu \epsilon_3\cdot\epsilon_4 + (2p_4+p_3)\cdot\epsilon_3\epsilon_4^\mu - (2p_3+p_4)\cdot\epsilon_4\epsilon_3^\mu.$$

APPENDIX B: SOLUTION OF THE NEUTRINO MOMENTA

We give here briefly the method of solving the neutrino momenta in Eqs. (45). Let $p_{l_1^+} = p_l$, $p_{l_2^-} = p_l'$, $p_{\bar{b}} = p_b'$, $p_{\nu_1} = (E,X,Y,Z)$, $p_{\nu_2} = (E',X',Y',Z')$, $p_{lb} = p_l + p_b$, $p_{lb}' = p_l' + p_b'$, $p_0 = -(p_b + p_b' + p_l + p_l')$. Then we can get

$$X = aE + bZ + \delta, \quad Y = cE + dZ + \xi, \tag{B1}$$
$$X' = a'E' + b'Z' + \delta', \quad Y' = c'E' + d'Z' + \xi',$$

where

$$a = \frac{E_{lb}p_l^y - E_l p_{lb}^y}{\Delta_1}, \quad b = \frac{-p_{lb}^z p_l^y + p_l^z p_{lb}^y}{\Delta_1}, \tag{B2}$$
$$c = \frac{-E_{lb}p_l^x + E_l p_{lb}^x}{\Delta_1}, \quad d = \frac{p_{lb}^z p_l^x - p_l^z p_{lb}^x}{\Delta_1},$$
$$\delta = \frac{-(m_t^2 - p_{lb}^2)/2p_l^y + m_W^2/2p_{lb}^y}{\Delta_1}, \quad \xi = \frac{(m_t^2 - p_{lb}^2)/2p_l^x - m_W^2/2p_{lb}^x}{\Delta_1},$$
$$\Delta_1 = p_{lb}^x p_l^y - p_{lb}^y p_l^x,$$

and a',b',c',d',δ',ξ' are obtained from the above equations by the substitutions of momenta without $'$ to those with $'$. We further express E,E' in terms of Z,Z':

$$E = fZ + gZ' + h, \quad E' = f'Z + g'Z' + h', \tag{B3}$$

where

$$f = \frac{-bc' + da'}{\Delta_2}, \quad g = \frac{-b'c' + d'a'}{\Delta_2},$$
$$h = \frac{(p_0^x - \delta - \delta')c' + a'(p_0^y - \xi - \xi')}{\Delta_2}, \tag{B4}$$
$$f' = \frac{-ad + cb}{\Delta_2}, \quad g' = \frac{-ad' + cb'}{\Delta_2},$$
$$h' = \frac{(p_0^y - \xi - \xi')a + c(p_0^x - \delta - \delta')}{\Delta_2},$$
$$\Delta_2 = ac' - ca'.$$

Inserting the above expressions into $E^2 = X^2 + Y^2 + Z^2$, and $E'^2 = X'^2 + Y'^2 + Z'^2$, we get the following two quadratic equations for Z, Z':

$$AZ^2 + BZZ' + CZ'^2 + D + UZ + VZ' = 0, \tag{B5}$$

$$A'Z'^2 + B'ZZ' + C'Z^2 + D' + U'Z' + V'Z = 0, \tag{B6}$$

with

$$A = f^2 - 1 - (af+b)^2 - (cf+d)^2, \quad B = 2[fg - ag(af+b) - cg(cf+d)], \tag{B7}$$

$$C=g^2-a^2g^2-c^2g^2,\quad D=h^2-(ah+\delta)^2-(ch+\xi)^2,$$

$$U=2[fh-(ah+\delta)(af+b)-(ch+\xi)(cf+d)],$$

$$V=2[gh-ag(ah+\delta)-cg(ch+\xi)],$$

and A',B',C',D',U',V' can be gotten from the above equations by replacing the variables without $'$ with the ones with $'$ and interchanging f', g'.

Eqs. (B5) and (B6) can obviously give at most four real solutions for (Z,Z'). They can be solved by standard methods: solving Z' in Eq. (B5) as functions of Z, we get two expressions for Z', then inserting them separately into Eq. (B6), we shall get the same quartic equation of Z which has up to four real solutions. Although those solutions will be doubled when we calculate Z' with the two expressions obtained from Eq. (B5), half of them are false solutions to Eq. (B6).

APPENDIX C: ANALYSIS ON THE CONTAMINATIONS TO *CP*-VIOLATING EFFECTS IN *pp* COLLISION

We assume the partons inside the proton have no intrinsic transverse momenta and denote the parton level reaction as $a(x_1)\bar{a}(x_2)\to t\bar{t}$ with x_1 and x_2 being the Bjorken scale parameters. The hadronic level cross section can be written as

$$\begin{aligned} d\sigma &= 2f_a^p(x_1)f_{\bar{a}}^p(x_2)d\hat{\sigma}(a\bar{a}\to t\bar{t})dx_1dx_2/(1+\delta_{a,\bar{a}}) \\ &= \{[f_a^p(x_1)f_{\bar{a}}^p(x_2)+f_a^p(x_2)f_{\bar{a}}^p(x_1)]+[f_a^p(x_1)f_{\bar{a}}^p(x_2)-f_a^p(x_2)f_{\bar{a}}^p(x_1)]\}d\hat{\sigma}(a\bar{a}\to t\bar{t})/(1+\delta_{a,\bar{a}})dx_1dx_2, \end{aligned} \tag{C1}$$

where f_a^p, $f_{\bar{a}}^p$ are the parton distribution functions of a and $\bar{a}$ in proton. The function $F^+(x_1,x_2)=f_a^p(x_1)f_{\bar{a}}^p(x_2)+f_a^p(x_2)f_{\bar{a}}^p(x_1)$ is CP even (its CP transformation is just the interchanging of x_1, x_2), so that no contamination comes from it. Now we look at the function $F^-(x_1,x_2)=f_a^p(x_1)f_{\bar{a}}^p(x_2)-f_a^p(x_2)f_{\bar{a}}^p(x_1)$. Contaminations should come from $F^-(x_1,x_2)$ term since it is CP odd. $F^-(x_1,x_2)=0$ for $a=g$. There are no contaminations from the initial gluon reaction. All contaminations come from the initial quark reactions which are subdominant processes at the CERN LHC. There are nonzero CP-violating contaminations only when the observables contain asymmetry between x_1 and x_2. Since the Lorentz invariant observables can always be calculated in the center of mass frame of the parton which depends only on x_1x_2, they will receive no contaminations. Therefore, within the framework of the parton model, there are no contaminations to Lorentz invariant observables. In our study, they are f_2,O_1,O_l',O_2,O_4.

[1] Report of the tev2000 Study Group, edited by D. Amidei and R. Brock, Report No. FERMILAB-Pub-96/082, 1996.

[2] W. Hollik, W. M. Mösle, C. Kao, and D. Wackeroth, hep-ph/9711419, and references therein.

[3] C.S. Li, C.-P. Yuan, and H.Y. Zhou, Phys. Lett. B **424**, 76 (1998).

[4] H.E. Haber and G.L. Kane, Phys. Rep. **117**, 75 (1985); J.F. Gunion and H.E. Haber, Nucl. Phys. **B272**, 1 (1986); **B402**, 567 (1993).

[5] G.L. Kane, G.A. Landinsky, and C.-P. Yuan, Phys. Rev. D **45**, 124 (1992).

[6] C.R. Schmidt and M.E. Peskin, Phys. Rev. Lett. **69**, 410 (1992).

[7] C.R. Schmidt, Phys. Lett. B **293**, 111 (1992).

[8] D. Atwood, A. Aeppli, and A. Soni, Phys. Rev. Lett. **69**, 2754 (1992).

[9] A. Brandenburg and J.P. Ma, Phys. Lett. B **298**, 211 (1993).

[10] W. Bernreuther, O. Nachtmann, P. Overmann, and T. Schröder, Nucl. Phys. **B388**, 53 (1992).

[11] P. Haberl, O. Nachtmann, and A. Wilch, Phys. Rev. D **53**, 4875 (1996).

[12] W. Bernreuther and A. Brandenburg, Phys. Rev. D **49**, 4481 (1994).

[13] B. Grzadkowski, B. Lampe, and K.J. Abraham, Phys. Lett. B **415**, 193 (1997).

[14] S.Y. Choi, C.S. Kim, and Jabe Lee, Phys. Lett. B **415**, 67 (1997).

[15] Particle Data Group, R.M. Barnett *et al.*, Phys. Rev. D **54**, 1 (1996).

[16] S. Bar-Shalom, D. Atwood, and A. Soni, Phys. Rev. D **57**, 1495 (1998).

[17] J.M. Yang and C.S. Li, Phys. Rev. D **52**, 1541 (1995); C.S. Li, B.Q. Hu, J.M. Yang, and C.G. Hu, *ibid.* **52**, 5014 (1995); **53**, 4112(E) (1996); C.S. Li, H.Y. Zhou, Y.L. Zhu, and J.M. Yang, Phys. Lett. B **379**, 135 (1996); J.M. Yang and C.S. Li, Phys. Rev. D **54**, 4380 (1996).

[18] J. Kim, J.L. Lopez, D.V. Nanopoulos, and R. Rangarajan, Phys. Rev. D **54**, 4364 (1996); S. Catani *et al.*, Phys. Lett. B **378**, 329 (1996); T. Gehrmann *et al.*, *ibid.* **381**, 221 (1996); J.A. Coarasa *et al.*, Eur. Phys. J. **C2**, 373 (1998); S. Frixione, in *Heavy Flavours II*, edited by A. J. Buras and M. Lindner (World Scientific, Singapore, 1995), hep-ph/9702287.

[19] H.Y. Zhou, C.S. Li, and Y.P. Kuang, Phys. Rev. D **55**, 4412 (1997); H.Y. Zhou and C.S. Li, *ibid.* **55**, 4421 (1997).
[20] K. Hagiwara and D. Zeppenfeld, Nucl. Phys. **B313**, 560 (1989); V. Barger, T. Han, and D. Zeppenfeld, Phys. Rev. D **41**, 2782 (1990).
[21] W. Hollik, Fortschr. Phys. **38**, 165 (1990); A Denner, *ibid.* **41**, 307 (1993).
[22] G.C. Branco and M.N. Rebelo, Phys. Lett. **160B**, 117 (1985); S. Weinberg, Phys. Rev. D **42**, 860 (1990).
[23] W. Bernreuther, T. Schröder, and T.N. Pham, Phys. Lett. B **279**, 389 (1992).
[24] M. Aoki and N. Oshimo, hep-ph/9801294.
[25] G.L. Kane, J. Pumplin, and W. Repko, Phys. Rev. Lett. **41**, 1689 (1978); A. Devoto, G.L. Kane, J. Pumplin, and W. Repko, *ibid.* **43**, 1062 (1979); **43**, 1540 (1979); Phys. Lett. **90B**, 436 (1980).
[26] J.F. Donoghue and G. Valencia, Phys. Rev. Lett. **58**, 451 (1987).
[27] D. Chang, W.-Y. Keung, and I. Phillips, Nucl. Phys. **B408**, 286 (1993).
[28] G.A. Ladinsky and C.-P. Yuan, Phys. Rev. D **49**, 4415 (1994).
[29] K. Hagiwara *et al.*, Nucl. Phys. **B282**, 253 (1987); W. Bernreuther and O. Nachtmann, Phys. Lett. B **268**, 424 (1991).
[30] D. Atwood and A. Soni, Phys. Rev. D **45**, 2405 (1992).
[31] M. Dovier, L. Duflot, F. Le Diberder, and A. Rougé, Phys. Lett. B **306**, 411 (1993).
[32] M. Diehl and O. Nachtmann, Z. Phys. C **62**, 397 (1994); Eur. Phys. J. **C1**, 177 (1998).
[33] J.H. Kühn, Phys. Lett. B **313**, 458 (1993), and references therein.
[34] G.A. Landsky, Phys. Rev. D **46**, 3789 (1992); **47**, 3086(E) (1993).
[35] A.D. Martin, W.J. Stirling, and R.G. Roberts, Phys. Lett. B **354**, 155 (1995).
[36] H.L. Lai, J. Huston, S. Kuhlmann, F. Olness, J. Owens, D. Soper, W.K. Tung, and H. Weerts, Phys. Rev. D **55**, 1280 (1997).
[37] S. Dawson, hep-ph/9612229; J.F. Grivaz, Nucl. Phys. B (Proc. Suppl.) **64**, 138 (1998).
[38] G. Passarino and M. Veltman, Nucl. Phys. **B160**, 151 (1979); G. 't Hooft and M. Veltman, *ibid.* **B153**, 365 (1979).